
MeanSparse: Post-Training Robustness Enhancement Through Mean-Centered Feature Sparsification

Sajjad Amini^{1,2}, Mohammadreza Teymorianfar¹, Shiqing Ma¹, Amir Houmansadr¹

¹University of Massachusetts Amherst, ²Sharif University of Technology
 {samini, mteymorianf, shiqingma}@umass.edu, amir@cs.umass.edu

Abstract

We present a simple yet effective method to improve the robustness of Convolutional Neural Networks (CNNs) against adversarial examples by post-processing an adversarially trained model. Our technique, MEANSPARSE, cascades the activation functions of a trained model with novel operators that sparsify mean-centered feature vectors. This is equivalent to reducing feature variations around the mean, and we show that such reduced variations merely affect the model’s utility, yet they strongly attenuate the adversarial perturbations and decrease the attacker’s success rate. Our experiments show that, when applied to the top models in the RobustBench leaderboard, MEANSPARSE achieves a new robustness record of 72.08% (from 71.07%) and 59.64% (from 59.56%) on CIFAR-10 and ImageNet, respectively, in terms of AutoAttack accuracy. Code is available at <https://github.com/SPIN-UMass/MeanSparse>

1 Introduction

Adversarial Training (AT) [26] has become a popular method to defend deep neural networks (DNNs) against adversarial examples [38, 15]. The core idea involves generating adversarial examples during the training phase and incorporating them into the training dataset. The mere existence of such adversarial examples are due to features that are non-robust to imperceptible changes [20]. AT attenuates the significance of these non-robust features on model’s output, therefore improving robustness.

While AT has demonstrated effectiveness in enhancing model robustness, it faces limitations in generalizability across various methods for generating adversarial examples and suffers from low training efficiency. Various directions have been taken [49, 17, 47] to overcome these challenges in order to enhance the robustness provided by AT. In this work, we explore a complementary direction towards improving AT’s robustness: The design of activation functions presents a promising, yet underexplored, avenue for improving AT. Smooth Adversarial Training (SAT) has shown that replacing ReLU with a smooth approximation can enhance robustness [48], and activation functions with learnable parameters have also demonstrated improved robustness in adversarially trained models [9, 35]. This paper aims to further investigate the potential of activation functions in enhancing AT, providing new insights and approaches to bolster model robustness.

In this work, we explore the impact of sparsifying features to enhance robustness against adversarial examples. We introduce the MEANSPARSE technique, which integrates sparsity into models trained using AT. Our findings indicate that non-robust features persist in the model, albeit with reduced values, even after applying AT. This insight inspired our approach to partially block these remaining non-robust features. To achieve this, we propose imposing sparsity over mean-centered features, denoted by *Mean-based Sparsification*, inspired by sparsity-promoting regularizers commonly used for feature denoising [12, 1] and feature selection [40, 27].

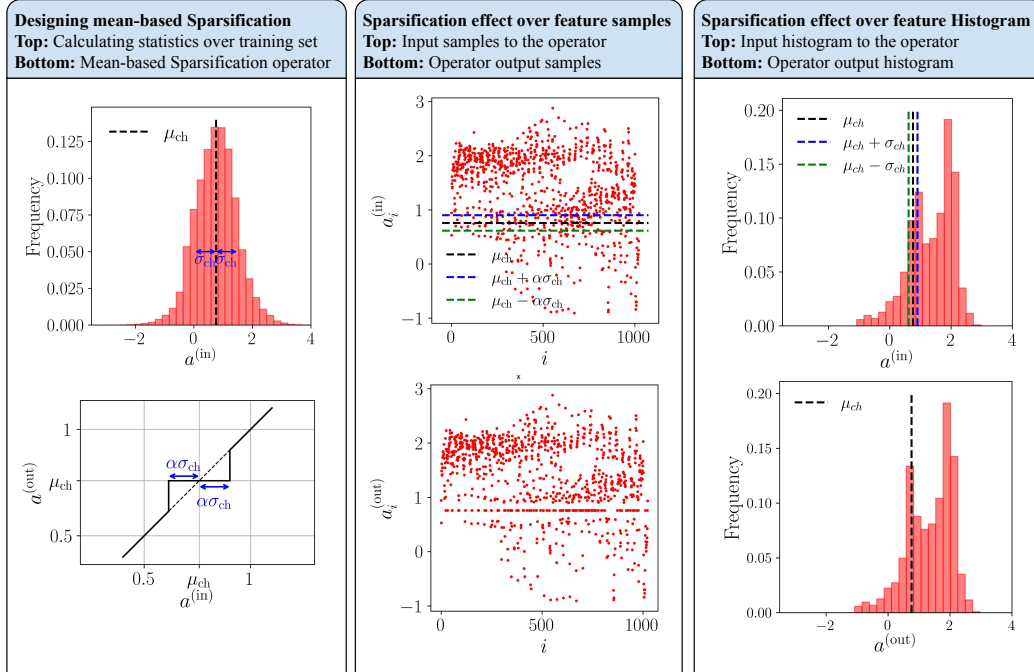


Figure 1: Mean-based sparsification operator used in the MeanSparse technique for hypothetical channel ch . The first column represents the design procedure. First, the mean (μ_{ch}) and standard deviation (σ_{ch}) are calculated over the training set (top figure). The mean-based sparsification operator is designed with hyper-parameter α which blocks the variations in the $\alpha\sigma_{ch}$ vicinity of μ_{ch} (bottom figure). The second column represents how mean-based sparsification affects the input features for one test sample (top figure) and generates output features (bottom figure). The effect of mean-based sparsification over the feature histogram is also demonstrated in the third column.

Figure 1 illustrates the mean-based sparsification operator, a crucial component of the MeanSparse technique. In the first column, the histogram for a randomly selected channel in the first layer of the RaWideResNet trained on the CIFAR-10 dataset [31] is displayed, showing the mean and standard deviation calculated over the CIFAR-10 training set (top figure). The mean-based sparsification operator (bottom figure), parameterized by α blocks variations around the mean. In the second column, the top figure shows the features of a hypothetical channel for a CIFAR-10 test image. The sparsification operator blocks variations between the blue and green dashed lines, producing the output shown in the bottom figure. The third column provides a similar visualization for the input and output histograms of the sparsification operator. Blocking high-probability (low information) variations prevents deterioration of model performance while limiting the attacker’s ability to exploit that region.

MeanSparse establishes new state-of-the-art robustness. Applying it to the leading robust model on CIFAR-10 increases ℓ_∞ AutoAttack accuracy from 71.07% to 72.08%, while clean accuracy remains nearly unchanged (93.27% to 93.24%) [7]. On ImageNet-1K, MeanSparse boosts the AutoAttack accuracy of the third-ranked model to 59.64%, surpassing the previous best of 59.56%, according to RobustBench specifications[10, 7].

In summary, we make the following contributions:

- Integrating MeanSparse into the top two robust models from the RobustBench benchmark [7] enhanced robustness, setting a new record on CIFAR-10 (71.07% to 72.08%). Additionally, applying MeanSparse to the third-ranked ImageNet model set a new AutoAttack accuracy record (59.56% to 59.64%).
- The developed MeanSparse technique can be easily integrated into trained models, enhancing their robustness at almost no additional cost.

- We identified critical limitations of current activation functions and developed MeanSparse to mitigate these limitations. Our simulations show that regardless of the activation function, MeanSparse improves robustness upon integration.
- Through various experiments, we demonstrated that the improved robustness resulting from MeanSparse can be generalized across different model sizes and architecture types.

2 Preliminaries

2.1 Notations

We use bold lowercase letters to show vectors while the i -th element of vector \mathbf{x} is represented by x_i . Two vector norm metrics are used throughout the paper, including $\ell_0 = \|\cdot\|_0$ (number of non-zero elements) and $\ell_2 = \|\cdot\|_2$ (Euclidean norm). The ℓ_0 norm can also effectively penalize the variables with small values but its nonsmoothness limits its application. The proximal operator finds the minimizer of function f in the vicinity of input vector \mathbf{v} and plays an essential role in our intuition to design the mean-based sparsification operator.

Definition 2.1 (Proximal operator [30]). Let $f : \mathbb{R}^n \rightarrow \mathbb{R} \cup \{+\infty\}$ be a proper and lower semi-continuous function. The proximal operator (mapping) $\text{prox}_f : \mathbb{R}^n \rightarrow \mathbb{R}^n$ of f at \mathbf{v} is defined as:

$$\text{prox}_f(\mathbf{v}) = \underset{\mathbf{x}}{\text{argmin}}_f f(\mathbf{x}) + \frac{1}{2}\|\mathbf{x} - \mathbf{v}\|_2^2 \quad (1)$$

The definition of proximal operator can be extended to nonsmooth functions such as ℓ_0 norm. Assume $f(\mathbf{a}) \triangleq \lambda\|\mathbf{a}\|_0$. Then the proximal operator can be calculated as [11]:

$$\text{prox}_f(\mathbf{v}) = \mathcal{H}_{2\lambda}(\mathbf{v}), \quad \mathcal{H}_\alpha(v) = \begin{cases} v & |v| > \sqrt{\alpha} \\ 0 & |v| \leq \sqrt{\alpha} \end{cases} \quad (2)$$

where $\mathcal{H}_\alpha(\cdot)$ is the element-wise hard-thresholding operator.

2.2 Related Work

Adversarial training, a method to enhance model robustness, encounters high complexity because of the adversarial attack design incorporated during training. The concept of using adversarial samples during training was first introduced in [38] and then AT was introduced in [26]. *Fast Gradient Sign Method* (FGSM) is a low-complexity attack design used for AT [41, 25, 47, 42]. This approach while reducing the complexity of AT, cannot generalize to more complex adversarial attacks. On the other hand using *Projected Gradient Descent* with AT, although increasing the attack design complexity due to its iterative nature, can better generalize to other adversarial attacks [26, 41, 44, 4]. *Curriculum Adversarial Training* gradually increases the complexity of adversarial samples during AT [2]. Other types of adversarial attacks also have been proposed to be used for AT including *Jacobian-based Saliency Map Attack* [32], Carlini and Wagner attack [3, 46] and attacking Ensemble of methods during AT [29], among others.

Different activation functions have been proposed that generally target to improve the generalizability of DNNs [14, 5, 34, 18, 22, 23, 13, 19]. Bounded ReLU (BReLU) where the output of ReLU is clipped to avoid adversarial perturbation propagation has shown robustness improvements in standard training scenarios [50]. The effect of symmetric activation functions [52], data-dependent activation functions [43], learnable activation functions [39] and activation function quantization [33] over the robustness of the model in standard training scenario have also been explored.

The performance of different non-parametric activation functions in the AT scenario is explored in [16] and smooth activation functions demonstrated better robustness. This result is on par with SAT where the authors argued that the ReLU activation function limits the robustness performance of AT due to its non-smooth nature. In other words, the non-smooth nature of ReLU makes the adversarial sample generation harder during training. Thus they proposed the SAT which replaces ReLU with its smooth approximation and trained using Adversarial training. The results show improved robustness while preserving the accuracy [48]. The effect of non-parametric activation function curvature has also been studied which shows that lower curvature improves the robustness [37].

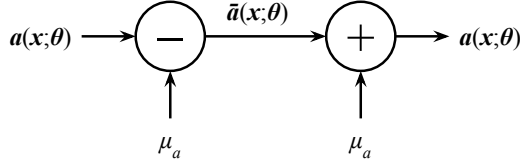


Figure 2: Mean-centered feature used in regularized optimization problem (3)

Parametric activation functions increase the flexibility of activation functions while the parameters can be learned during the training phase. This flexibility, if designed intelligently, is also shown to be effective in improving robustness with AT. An example of Parametric activation functions is parametric shifted SiLU (PSSILU) [9].

Similar to Neural Architecture Search (NAS), *Searching for Adversarial Robust Activation Functions* (SARAF) is designed to search over candidate activation functions to maximize the model robustness. Using a meta-heuristic search method, SARAF can handle the intractable complexity of the original search problem [36, 35].

3 Methodology

From the concept of non-robust features, it is understood that through adversarial training, these features become less informative about the output label [20]. From an information-theoretic point-of-view, we also recognize that as the occurrence probability of a random vector increases, its informational value decreases [6]. Consequently, to identify the less informative features, it is useful to examine the regions of high probability within the feature space. One easily accessible high-probability point is the feature mean. Following this reasoning, we can block minor variations around the mean to eliminate the less informative or equivalently, the non-robust features. We begin this section by designing a regularized optimization objective to block non-robust features. Although this optimization problem is not used in the final MeanSparse technique, its parameter update rule provides valuable insight into the design of the sparsification operator introduced later. Finally, we demonstrate the complete MeanSparse technique.

3.1 Intuition from Regularized Optimization Objective

The small changes around the feature mean value at the output of different layers are potentially non-robust features. Thus we start by penalizing those changes using ℓ_0 norm in an arbitrary layer l for a training sample \mathbf{x} (extension to the whole dataset and all layers is straightforward). The original training objective can be formulated as:

$$\mathcal{P}_0 : \boldsymbol{\theta}_0^* = \underset{\boldsymbol{\theta}}{\operatorname{argmin}} L(\boldsymbol{\theta}) + \gamma \|\bar{\mathbf{a}}(\mathbf{x}; \boldsymbol{\theta})\|_0, \quad L(\boldsymbol{\theta}) \triangleq \mathcal{L}(\mathbf{y}(\mathbf{x}), \mathbf{y}^*; \boldsymbol{\theta}) \quad (3)$$

where $\boldsymbol{\theta}$ is the vector containing model parameters, γ is a hyper-parameter, $\bar{\mathbf{a}}(\mathbf{x}; \boldsymbol{\theta})$ is the centralized feature vector before the activation function in the regularized layer, $\mathbf{y}(\cdot)$ is the model output and \mathbf{y}^* is the target label corresponding to \mathbf{x} . Throughout the paper, we assume μ_a to be a fixed vector that is updated using an exponential filter during training, similar to the mean and variance vectors calculated in a batch normalization layer. Figure 2 represents the way mean-centered features for regularization are generated. One option to solve the optimization problem in (3) is via the penalty method.

To solve problem (3), we introduce an approximate version of this problem based on the penalty method (for simplicity we use $\bar{\mathbf{a}}$ instead of $\bar{\mathbf{a}}(\mathbf{x}; \boldsymbol{\theta})$):

$$\mathcal{P}_\lambda : \boldsymbol{\theta}_{0,\lambda}^*, \mathbf{w}^* = \underset{\boldsymbol{\theta}, \mathbf{w}}{\operatorname{argmin}} L(\boldsymbol{\theta}) + \gamma \|\mathbf{w}\|_0 + \frac{1}{2\lambda} \|\mathbf{w} - \bar{\mathbf{a}}\|_2^2 \quad (4)$$

where λ is the penalty parameter, \mathbf{w} is the penalty variable, and the optimization is with respect to both variables $\boldsymbol{\theta}$ and \mathbf{w} . Based on the penalty method (PM), we can conclude:

$$\lim_{\lambda \rightarrow 0} \boldsymbol{\theta}_{0,\lambda}^* = \boldsymbol{\theta}_0^* \quad (5)$$

So to approximate θ_0^* , one can solve problem \mathcal{P}_λ and decrease λ during the training. One approach to solve problem \mathcal{P}_λ is to use block coordinate descent where the θ and w are updated sequentially [28]. So we have two steps in each training iteration k .

Step1 → **Calculating w_k** : To calculate w_k , we should solve:

$$w_k = \underset{w}{\operatorname{argmin}} \gamma\lambda\|w\|_0 + \frac{1}{2}\|w - \bar{a}_{k-1}\|_2^2 \quad (6)$$

The problem in (6) matches the definition of the proximal operator in (1) and can be solved exactly by the proximal operator for the function $f(w) = \gamma\lambda\|w\|_0$. Thus we have:

$$w_k = \underset{f}{\operatorname{prox}}(z_{k-1}) = \mathcal{H}_{2\lambda\gamma}(\bar{a}_{k-1}) \quad (7)$$

Step 2 → **Calculating θ_k** : To calculate θ_k , we have to solve the following problem:

$$\theta_k = \underset{\theta}{\operatorname{argmin}} L(\theta) + \frac{1}{2\lambda}\|w_k - \bar{a}\|_2^2 \quad (8)$$

while w_k is calculated using hard-thresholding operator as in (7). One step of (stochastic) gradient descent can be used to update θ based on (8).

3.2 Mean-centered Feature Sparsification

Update rule (8) shows \bar{a} approaches $\mathcal{H}_{2\mu\gamma}(\bar{a}_{k-1})$ by the second term while the weight for this term is increasing (equivalently μ is decreasing) during the training. Based on this intuition, we propose to use the $\mathcal{H}_{2\mu\gamma}(\bar{a}_{k-1})$ in the forward propagation of the model. If we add the element-wise mean subtraction and addition in 2 into the hard-thresholding operator, we achieve the curve in the bottom of the first column in 1 assuming $\alpha\sigma_{\text{ch}} = (2\mu\lambda)^2$ (for simplicity of notation, we use Th instead). This curve represents a sparsification around the feature mean value μ_a . In other words, we have the following element-wise operation over the input $a^{(\text{in})}$:

$$a^{(\text{out})} = \begin{cases} \mu_a & \text{if } |a^{(\text{out})} - \mu_a| \leq Th \\ a^{(\text{in})} & \text{if } |a^{(\text{out})} - \mu_a| > Th \end{cases}$$

So, features within the Th -vicinity of the feature mean are blocked and the mean value is output, while larger values pass through the Sparsification operator unchanged.

3.3 MeanSparse Technique

Now we have a mean-centered sparsification operator that can be integrated into the model to block non-robust variations around the mean value. However, there are several challenges and improvements to address, which will be discussed in this section. By applying these enhancements, the final technique is formed.

Sparsification in Post-processing

As a general input-output mapping relation, mean-centered feature sparsification can be added to any part of deep learning architecture without changing the dimension. The back-propagation of training signals through this sparsification operator will be zero for inputs in the Th -vicinity of the feature mean, which avoids model training since the mean is the place where the highest rate of features lies. Two options can be applied to solve this problem.

The first approach is to gradually increase the Th value through iterations. At the start of training, Th is set to zero. Thus, sparsification reduces to an identity transformation, which solves the problem of backpropagation. Then, throughout the iterations, Th is increased until it reaches a predefined maximum value. The most challenging problem in this scenario is the selection of a Th scheduler as the model output is not differentiable with respect to Th and Th cannot be updated using gradient. In this scenario, we need to calculate the mean vector for the input feature representation inside the sparsification operator in a similar way to batch normalization layers.

The second solution is to apply sparsification as a post-training step to an adversarially trained model. In this scenario, first, we freeze the model weights and add the mean-centered feature sparsification

operator to the model in the predefined positions. Then we need to pass through the complete training set once to calculate the feature mean value. Next, we decide on the value of Th . Similar to the previous scenario, this step cannot be done using gradient-based methods as the operator is not differentiable with respect to Th . Thus, we can search over a range of Th values and find the best one that results in the highest robustness while maintaining the model’s clean accuracy.

In this paper, we use the second method. Thus, we freeze the model and apply sparsification over mean-centered features before the activation functions in the trained model. Then calculate the mean value over the training set and finally find the value of Th that results in the best robustness performance while maintaining the model’s clean accuracy.

Adaptive Sparsification Using Feature Standard Deviation

As we need to apply sparsification before all activations in the model, searching over a simple space and finding a suitable set of Th for different activation functions becomes intractable, even in small models. Thus, we design to select the threshold as $Th = \alpha \times \sigma_a$. While we pass through the training set to find the mean value μ_a , we can also determine the variance value σ_a^2 in parallel and use $Th = \alpha \times \sigma_a$ as the threshold. As a result, for a fixed value of α , the blocking vicinity around the mean increases as the variance of the feature increases.

Per-channel Sparsification

Throughout the neural network, the input to the activation functions can be considered as 4-dimensional, represented as $N \times C \times H \times W$. To better capture the statistics in the representation, we use per-channel mean μ_{ch} and variance σ_{ch} in sparsification operator. As a result, the mean and variance vectors are C -dimensional vectors. The sparsification operates on each feature channel separately, using the mean and variance of the corresponding channel.

Complete Pipeline

The complete pipeline to apply MeanSparse technique is formed by equipping the mean-centered sparsification operator with the three aforementioned modifications and adding it before all activation functions in the model with a shared α parameter. Figure 1 illustrates an example of integrating the MeanSparse technique into an adversarially trained model. In the first column, the upper figure represents the histogram of one channel features in the first layer of RaWideResNet trained adversarially over the CIFAR-10 dataset [31] along with the mean μ_{ch} and standard deviation σ_{ch} over the complete training set. Based on this histogram, we design the bottom sparsification operator where the variations in $\alpha\sigma_{ch}$ -vicinity of the mean are blocked. The second and third column represents the input and output of the sparsification operator for one test image of the CIFAR-10 dataset x_t in sample space and histogram, respectively. The top figures are input and the bottom ones are output. The feature histogram for x_t is bimodal. One of the modes matched the μ_{ch} which is the feature’s peak over the training set. Based on our intuition, the variations in this region are uninformative and can be blocked as we see in the bottom figures of the second and third columns.

By using the MeanSparse presented in this paper, one can enhance the state-of-the-art robust accuracy over both CIFAR-10 [21] and ImageNet [10] datasets, as evidenced by the RobustBench [7] rankings. Through various ablation studies, we also demonstrate the effectiveness of the proposed pipeline in multiple scenarios. This pipeline sheds light on a new approach to improve robustness without compromising clean accuracy.

4 Experiments

The proposed pipeline in Figure 1 represents the way one can integrate MeanSparse into different trained models. In this section, we present several experiments to demonstrate the effectiveness of the MeanSparse across different architectures and datasets and in improving the state-of-the-art robustness. The experiments were conducted using an NVIDIA A100 GPU.

4.1 Evaluation Metrics

Throughout the experiments, we use *Clean* to represent the model accuracy for clean data. $A\text{-}PGD_{ce}$ is used as a robustness measure and represents accuracy after applying Auto PGD with Cross-Entropy (CE) loss. $A\text{-}PGD$ is used as another robustness measure and represents accuracy after applying Auto-PGD with both CE and Difference of Logits Ratio (DLR) loss metrics. Finally, we use *AA* to represent AutoAttack accuracy. All the robustness metrics can be found in [8]. In our experiments, MeanSparse is applied post-training, eliminating the randomness typically introduced during training. Moreover, results from RobustBench for $A\text{-}PGD_{ce}$, $A\text{-}PGD$, and *AA* accuracies are highly consistent, showing negligible variability. Consequently, statistical significance tests are almost zero for all the results reported in this section.

4.2 Integration to State-of-the-Art Models

With the introduction of adversarial examples for deep learning models, their reliability was severely questioned [3]. However, several models have now been developed that present a high level of accuracy while also maintaining acceptable robustness against attacks imperceptible to humans [7]. In this part, we focus on the trained models with leading performance over CIFAR-10 [21] and ImageNet [10] datasets. We use the trained models and the proposed pipeline to integrate MeanSparse before all the activation functions. Then we evaluate the performance of the resulting models.

Table 1 presents the results of integrating MeanSparse into RaWideResNet [31] and WideResNet [45] architectures trained on the CIFAR-10 dataset and ConvNeXt-L [24] and RaWideResNet [31] on the ImageNet-1K dataset using adversarial training. The results are provided for different values of α (note that the threshold equals $\alpha \times \sigma_{ch}$). RaWideResNet [31] achieves the highest AA for ℓ_∞ untargeted attacks to the CIFAR-10 dataset submitted to RobustBench [7], while WideResNet [45] ranks second. The experiment results over the CIFAR-10 test set depict that for a range of α below 0.25, the clean accuracy has decreased negligibly or almost unchanged while $APGD_{ce}$ is increasing. Although these results may be attributed to overfitting, the result over the CIFAR-10 training set also represents a similar trend. So an important takeaway from CIFAR-10 results in Table 1 is that the variations around the mean value of representation can be considered as a capacity provided by the model for the attackers while its utilization is limited. MeanSparse requires one pass over CIFAR-10 training set to calculate the statistics. The time for this pass is 102 seconds and 95 seconds for the RaWideResNet and WideResNet architectures, respectively. The increase in $APGD_{ce}$ evaluation time after MeanSparse integration is negligible, with only a 2% increase in time.

If this capacity is controlled suitably, then the robustness of the model will be increased (model capacity for attacker will be decreased) while model utilization will be unchanged. So by increasing α from zero, we decrease the attacker capacity while user utilization is unchanged. By increasing α to larger values, we start to decrease user utilization, too. Although there is no rigid margin between these two cases, one can find suitable α values that limit the attacker side while user utilization is unchanged.

Results over ImageNet-1K presented in Table 1 show that similar outcomes are achieved when MeanSparse is integrated into models based on the ConvNeXt-L [24] and RaWideResNet [31] architectures adversarially trained. ConvNeXt-L [24] achieves the third-highest AA on the ImageNet-1K dataset for ℓ_∞ untargeted attacks submitted to RobustBench [7], while RaWideResNet [31] ranks eleventh. Note that throughout our experiment over the RaWideResNet [31] architecture for both CIFAR-10 and ImageNet-1k datasets, we do not apply the sparsification operator inside the Squeeze-and-Excitation module. The time for the MeanSparse pass over the ImageNet-1K training set is 89 minutes for the ConvNeXt-L architecture and 101 minutes for the RaWideResNet architecture. The increase in $APGD_{ce}$ evaluation time after MeanSparse integration is also negligible, with only a 3% increase in time.

One comment regarding Table 1 is that the results may not generalize well across attacks other than $APGD_{ce}$. Therefore, in the next experiment, we evaluate AA as a complete suite of attacks for the values of α whose results are colored in blue in Table 1.

Figure 3(a) depicts the results for the Clean and AA metrics of the standard and MeanSparse-integrated versions of the RaWideResNet [31] and WideResNet [45] models, with α values set at 0.25 and 0.20 for the former and latter, respectively. RaWideResNet [31] currently holds the state-of-the-art performance in the RobustBench ranking [8] for ℓ_∞ untargeted attack. After post-processing with

Table 1: Clean accuracy and accuracy under A-PGD-CE attack [8] (represented by APGD_{ce}) for leading robust models on the CIFAR-10 and ImageNet-1k datasets (*Base* row) and after their integration with the MeanSparse technique (RaWideResNet [31] and WideResNet [45] are ranked 1st and 2nd, respectively, on Robustbench for CIFAR-10 dataset and ConvNeXt-L [24] and RaWideResNet [31] are ranked 3rd and 11th, respectively, on Robustbench [7]). The best result in each column is in **bold** and the threshold selected through the proposed pipeline is in **blue**.

α	CIFAR-10								ImageNet-1k			
	RaWideResNet [31]				WideResNet [45]				ConvNeXt-L [24]		RaWideResNet [31]	
	Train		Test		Train		Test		Test		Test	
	Clean	APGD _{ce}	Clean	APGD _{ce}	Clean	APGD _{ce}	Clean	APGD _{ce}	Clean	APGD _{ce}	Clean	APGD _{ce}
Base	99.15	93.44	93.27	73.87	99.37	94.69	93.26	73.45	78.02	60.28	73.58	52.24
0.15	99.15	93.69	93.27	74.40	99.36	94.94	93.15	73.92	78.00	60.62	73.24	53.38
0.20	99.13	93.75	93.26	74.52	99.33	94.93	93.18	74.11	78.04	60.88	73.28	53.78
0.25	99.10	93.71	93.24	74.74	99.32	94.85	93.03	74.12	77.94	61.12	72.82	53.92
0.30	99.07	93.49	93.17	74.63	99.29	94.58	92.90	74.04	77.96	61.48	72.36	53.86
0.35	98.98	93.12	93.04	74.55	99.23	94.07	92.75	73.72	77.74	61.54	71.74	52.92
0.40	98.87	92.48	92.88	73.90	99.11	93.27	92.38	73.32	77.56	61.84	69.90	51.68
0.45	98.70	91.37	92.60	73.36	98.92	91.93	92.08	72.27	77.12	62.18	67.16	48.74
0.50	98.42	89.76	92.37	72.37	98.66	90.17	91.55	71.10	76.90	62.32	61.78	43.06

the proposed pipeline, the Clean accuracy drops slightly (from 93.27% to 93.24%), while the AA significantly increases (from 71.07% to 72.08%), setting a new record for robustness in terms of AA on the CIFAR-10 dataset. Similar results can be obtained for WideResNet [45]. Also, as a result of post-processing the robust model based on the WideResNet architecture, the resulting AA accuracy (71.40%) exceeds this value for the robust model based on the RaWideResNet architecture (71.04%), even though WideResNet has a less complex architecture compared to RaWideResNet, which is equipped with the Squeeze-and-Excitation module.

Figure 3(b) illustrates the clean and AA accuracy for two different models adversarially trained on the ImageNet-1k dataset. By carefully selecting the α value, while the Clean accuracy remains unchanged, the AA accuracy improves significantly. Although the ConvNeXt-L model [24] currently ranks third in AA accuracy for ℓ_∞ untargeted attacks, after postprocessing with the proposed pipeline, its AA accuracy rises to 59.64% from 58.48%. This result surpasses the current first-ranked model, which is based on the Swin-L architecture and adversarially trained [24], and has an AA accuracy of 59.56%.

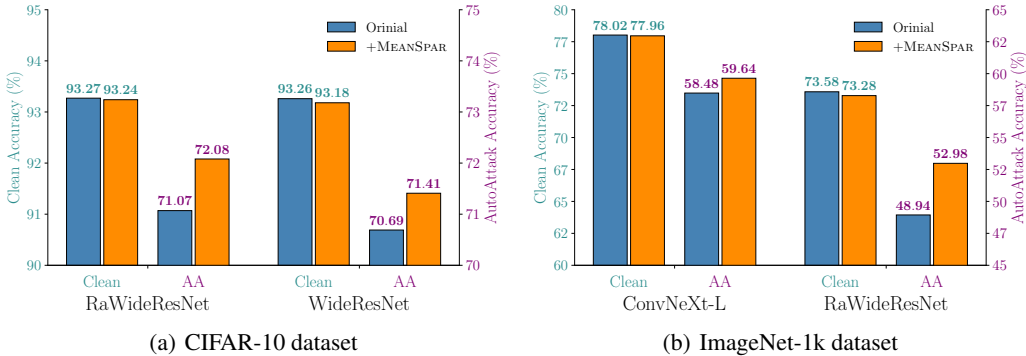


Figure 3: Original models performance along with their performance after integrating with MeanSparse technique (for CIFAR-10 dataset we have RaWideResNet [31] and WideResNet [45] architecture which are ranked 1st and 2nd, respectively, on Robustbench while for ImageNet-1k we have ConvNeXt-L [24] and RaWideResNet [31] that ranked 3rd and 11th, respectively, on Robustbench [7])

4.3 Insights from Ablation Study

We conducted several experiments to explore different aspects of MeanSparse integration into trained models. These experiments examine the effects of activation functions A.1, the type of adversarial attack (either ℓ_∞ or ℓ_2) A.2, the types of adversarial examples used during training with AT A.3, the impact of centering MeanSparse around the mean value A.4, the influence of attack power on MeanSparse integration performance A.5, and the effects of integrating MeanSparse with different patterns, such as isolated integration with a single activation A.6. The main takeaways from our ablation study can be summarized as:

- MeanSparse effectively enhances robustness across various activation functions. In other words, the activation function alone does not effectively eliminate non-robust features, which are previously reduced during training.
- MeanSparse is effective against both ℓ_∞ and ℓ_2 attacks. Specifically, if a model is fortified against ℓ_∞ attacks using AT, adding MeanSparse enhances robustness against both ℓ_∞ and ℓ_2 attacks. Also, MeanSparse is not sensitive to the method used to generate adversarial samples during AT.
- Using dedicated mean and variance for each channel in the MeanSparse technique is critical to its performance. Otherwise, we cannot expect the observed improvement in robustness.
- Integrating MeanSparse in isolated activation functions remains effective for robustification, although the improvement is limited.
- Although we have several results showing performance improvements in convolutional neural networks (CNNs), the integration of MeanSparse into attention-based architectures is still under consideration. In our initial experiment, we have not observed results on par with those in CNN-based architectures.

4.4 Limitations

The MeanSparse technique proposed in this paper is a post-training method that is useful on top of adversarially trained models. Using MeanSparse for models trained in a standard way does not lead to robustness improvement as we expect based on our intuition introduced in this paper. The current version of the MeanSparse technique has been applied to convolutional neural networks, and we still have not achieved comparable results on attention-based architectures. The current work explores the performance of the MeanSparse technique on the CIFAR-10 and ImageNet-1k datasets, which can be extended in future works.

5 Conclusions

Adversarial training, a widely accepted defense against evasion attacks, attenuates non-robust feature extractors in a model. Although adversarial training (AT) is effective, this paper demonstrates that there is still an easily accessible capacity for attackers to exploit. We introduce the MeanSparse technique, which partially blocks this capacity in the model available to attackers and enhances adversarial robustness. This technique, easily integrable after training, improves robustness without compromising clean accuracy. By integrating this technique into trained models, we achieve a new record in adversarial robustness against ℓ_∞ untargeted attacks on both CIFAR-10 and ImageNet-1k datasets.

Ethical Considerations

This research is conducted with adherence to the highest ethical standards, ensuring compliance with all relevant institutional and international guidelines to the best of the authors' knowledge. We critically assessed the societal impacts of our work, aiming to mitigate any negative consequences while promoting beneficial applications. Positive impacts include improved model robustness and increased trust in AI systems. Negative impacts involve potential misuse for malicious applications and reinforcing existing biases. To address these, we suggest mitigation strategies such as implementing gated releases, conducting fairness audits, and promoting transparency through public availability of code and data. Transparency and accountability were prioritized throughout the research process, and there were no conflicts of interest influencing the outcomes of this study.

References

- [1] Michal Aharon, Michael Elad, and Alfred Bruckstein. K-svd: An algorithm for designing overcomplete dictionaries for sparse representation. *IEEE Transactions on Signal Processing*, 54(11):4311–4322, 2006.
- [2] Qi-Zhi Cai, Chang Liu, and Dawn Song. Curriculum adversarial training. In *Proceedings of the 27th International Joint Conference on Artificial Intelligence*, pages 3740–3747, 2018.
- [3] Nicholas Carlini and David Wagner. Towards evaluating the robustness of neural networks. In *2017 IEEE Symposium on Security and Privacy (SP)*, pages 39–57. Ieee, 2017.
- [4] Minhao Cheng, Qi Lei, Pin-Yu Chen, Inderjit Dhillon, and Cho-Jui Hsieh. Cat: Customized adversarial training for improved robustness. In *IJCAI*, 2022.
- [5] Djork-Arné Clevert, Thomas Unterthiner, and Sepp Hochreiter. Fast and accurate deep network learning by exponential linear units (elus). *arXiv preprint arXiv:1511.07289*, 2015.
- [6] Thomas M. Cover and Joy A. Thomas. *Elements of Information Theory*. Wiley-Interscience, 2 edition, 2006.
- [7] Francesco Croce, Maksym Andriushchenko, Vikash Sehwal, Edoardo Debenedetti, Nicolas Flammarion, Mung Chiang, Prateek Mittal, and Matthias Hein. Robustbench: a standardized adversarial robustness benchmark. *arXiv preprint arXiv:2010.09670*, 2020.
- [8] Francesco Croce and Matthias Hein. Reliable evaluation of adversarial robustness with an ensemble of diverse parameter-free attacks. In *International conference on machine learning*, pages 2206–2216. PMLR, 2020.
- [9] Sihui Dai, Saeed Mahloujifar, and Prateek Mittal. Parameterizing activation functions for adversarial robustness. In *2022 IEEE Security and Privacy Workshops (SPW)*, pages 80–87. IEEE, 2022.
- [10] Jia Deng, Wei Dong, Richard Socher, Li-Jia Li, Kai Li, and Li Fei-Fei. Imagenet: A large-scale hierarchical image database. In *2009 IEEE Conference on Computer Vision and Pattern Recognition*, pages 248–255, 2009.
- [11] Michael Elad. *Sparse and Redundant Representations: From Theory to Applications in Signal and Image Processing*. Springer, 2010.
- [12] Michael Elad and Michal Aharon. Image denoising via sparse and redundant representations over learned dictionaries. *IEEE Transactions on Image Processing*, 15(12):3736–3745, 2006.
- [13] Stefan Elfving, Eiji Uchibe, and Kenji Doya. Sigmoid-weighted linear units for neural network function approximation in reinforcement learning. *Neural networks*, 107:3–11, 2018.
- [14] Xavier Glorot, Antoine Bordes, and Yoshua Bengio. Deep sparse rectifier neural networks. In *Proceedings of the fourteenth international conference on artificial intelligence and statistics*, pages 315–323. JMLR Workshop and Conference Proceedings, 2011.
- [15] Ian J Goodfellow, Jonathon Shlens, and Christian Szegedy. Explaining and harnessing adversarial examples. In *International Conference on Learning Representations (ICLR)*, 2014.
- [16] Sven Gowal, Chongli Qin, Jonathan Uesato, Timothy Mann, and Pushmeet Kohli. Uncovering the limits of adversarial training against norm-bounded adversarial examples. *arXiv preprint arXiv:2010.03593*, 2020.
- [17] Sven Gowal, Sylvestre-Alvise Rebuffi, Olivia Wiles, Florian Stimberg, Dan Andrei Calian, and Timothy A Mann. Improving robustness using generated data. *Advances in Neural Information Processing Systems*, 34:4218–4233, 2021.
- [18] Kaiming He, Xiangyu Zhang, Shaoqing Ren, and Jian Sun. Delving deep into rectifiers: Surpassing human-level performance on imagenet classification. In *Proceedings of the IEEE international conference on computer vision*, pages 1026–1034, 2015.
- [19] Dan Hendrycks and Kevin Gimpel. Gaussian error linear units (gelus). In *6th International Conference on Learning Representations, ICLR 2018*, 2018.
- [20] Andrew Ilyas, Shibani Santurkar, Dimitris Tsipras, Logan Engstrom, Brandon Tran, and Aleksander Madry. Adversarial examples are not bugs, they are features. *Advances in neural information processing systems*, 32, 2019.

- [21] Alex Krizhevsky and Geoffrey Hinton. Learning multiple layers of features from tiny images. Technical Report TR-2009, University of Toronto, 2009.
- [22] Jianfei Li, Han Feng, and Ding-Xuan Zhou. Signrelu neural network and its approximation ability. *Journal of Computational and Applied Mathematics*, 440:115551, 2024.
- [23] Senwei Liang, Liyao Lyu, Chunmei Wang, and Haizhao Yang. Reproducing activation function for deep learning. *arXiv preprint arXiv:2101.04844*, 2021.
- [24] Chang Liu, Yinpeng Dong, Wenzhao Xiang, Xiao Yang, Hang Su, Jun Zhu, Yuefeng Chen, Yuan He, Hui Xue, and Shibao Zheng. A comprehensive study on robustness of image classification models: Benchmarking and rethinking. *arXiv preprint arXiv:2302.14301*, 2023.
- [25] Guanxiong Liu, Issa Khalil, and Abdallah Khreishah. Using single-step adversarial training to defend iterative adversarial examples. In *Proceedings of the Eleventh ACM Conference on Data and Application Security and Privacy*, pages 17–27, 2021.
- [26] Aleksander Madry, Aleksandar Makelov, Ludwig Schmidt, Dimitris Tsipras, and Adrian Vladu. Towards deep learning models resistant to adversarial attacks. In *International Conference on Learning Representations*, 2018.
- [27] Julien Mairal, Rodolphe Jenatton, Guillaume Obozinski, and Francis Bach. Network flow algorithms for structured sparsity. In *Proceedings of the 27th International Conference on Machine Learning (ICML-10)*, pages 927–934, 2010.
- [28] Jorge Nocedal and Stephen J Wright. *Numerical optimization*. Springer, 1999.
- [29] Tianyu Pang, Kun Xu, Chao Du, Ning Chen, and Jun Zhu. Improving adversarial robustness via promoting ensemble diversity. In *International Conference on Machine Learning*, pages 4970–4979. PMLR, 2019.
- [30] Neal Parikh and Stephen Boyd. Proximal algorithms. *Foundations and Trends® in Optimization*, 1(3):127–239, 2014.
- [31] ShengYun Peng, Weilin Xu, Cory Cornelius, Matthew Hull, Kevin Li, Rahul Duggal, Mansi Phute, Jason Martin, and Duen Horng Chau. Robust principles: Architectural design principles for adversarially robust cnns. In *34th British Machine Vision Conference 2023, BMVC 2023, Aberdeen, UK, November 20-24, 2023*. BMVA, 2023.
- [32] Yi Qin, Ryan Hunt, and Chuan Yue. On improving the effectiveness of adversarial training. In *Proceedings of the ACM International Workshop on Security and Privacy Analytics*, pages 5–13, 2019.
- [33] Adnan Siraj Rakin, Jinfeng Yi, Boqing Gong, and Deliang Fan. Defend deep neural networks against adversarial examples via fixed and dynamic quantized activation functions. *arXiv preprint arXiv:1807.06714*, 2018.
- [34] Prajit Ramachandran, Barret Zoph, and Quoc V Le. Searching for activation functions. *arXiv preprint arXiv:1710.05941*, 2017.
- [35] Maghsood Salimi, Mohammad Loni, and Marjan Sirjani. Learning activation functions for adversarial attack resilience in cnns. In *International Conference on Artificial Intelligence and Soft Computing*, pages 203–214. Springer, 2023.
- [36] Maghsood Salimi, Mohammad Loni, Marjan Sirjani, Antonio Cicchetti, and Sara Abaspour Asadollah. Saraf: Searching for adversarial robust activation functions. In *Proceedings of the 2023 6th International Conference on Machine Vision and Applications*, pages 174–182, 2023.
- [37] Vasu Singla, Sahil Singla, Soheil Feizi, and David Jacobs. Low curvature activations reduce overfitting in adversarial training. In *Proceedings of the IEEE/CVF International Conference on Computer Vision*, pages 16423–16433, 2021.
- [38] Christian Szegedy, Wojciech Zaremba, Ilya Sutskever, Joan Bruna, Dumitru Erhan, Ian Goodfellow, and Rob Fergus. Intriguing properties of neural networks. *arXiv preprint arXiv:1312.6199*, 2013.
- [39] Mohammadamin Tavakoli, Forest Agostinelli, and Pierre Baldi. Splash: Learnable activation functions for improving accuracy and adversarial robustness. *Neural Networks*, 140:1–12, 2021.
- [40] Robert Tibshirani. Regression shrinkage and selection via the lasso. *Journal of the Royal Statistical Society: Series B (Methodological)*, 58(1):267–288, 1996.

- [41] Florian Tramèr, Alexey Kurakin, Nicolas Papernot, Ian Goodfellow, Dan Boneh, and Patrick McDaniel. Ensemble adversarial training: Attacks and defenses. In *International Conference on Learning Representations*, 2018.
- [42] BS Vivek and R Venkatesh Babu. Regularizers for single-step adversarial training. *arXiv preprint arXiv:2002.00614*, 2020.
- [43] Bao Wang, Alex Lin, Penghang Yin, Wei Zhu, Andrea L Bertozzi, and Stanley J Osher. Adversarial defense via the data-dependent activation, total variation minimization, and adversarial training. *Inverse Problems & Imaging*, 2020.
- [44] Yisen Wang, Xingjun Ma, James Bailey, Jinfeng Yi, Bowen Zhou, and Quanquan Gu. On the convergence and robustness of adversarial training. In *International Conference on Machine Learning*, pages 6586–6595. PMLR, 2019.
- [45] Zekai Wang, Tianyu Pang, Chao Du, Min Lin, Weiwei Liu, and Shuicheng Yan. Better diffusion models further improve adversarial training. In *International Conference on Machine Learning*, pages 36246–36263. PMLR, 2023.
- [46] Jing Wen, Lucas CK Hui, Siu-Ming Yiu, and Ruoqing Zhang. Dcn: detector-corrector network against evasion attacks on deep neural networks. In *2018 48th Annual IEEE/IFIP International Conference on Dependable Systems and Networks Workshops (DSN-W)*, pages 215–221. IEEE, 2018.
- [47] Eric Wong, Leslie Rice, and J Zico Kolter. Fast is better than free: Revisiting adversarial training. In *International Conference on Learning Representations*, 2019.
- [48] Cihang Xie, Mingxing Tan, Boqing Gong, Alan Yuille, and Quoc V Le. Smooth adversarial training. *arXiv e-prints*, pages arXiv–2006, 2020.
- [49] Yue Xing, Qifan Song, and Guang Cheng. Why do artificially generated data help adversarial robustness. *Advances in Neural Information Processing Systems*, 35:954–966, 2022.
- [50] Valentina Zantedeschi, Maria-Irina Nicolae, and Ambrish Rawat. Efficient defenses against adversarial attacks. In *Proceedings of the 10th ACM Workshop on Artificial Intelligence and Security*, pages 39–49, 2017.
- [51] Hongyang Zhang, Yaodong Yu, Jiantao Jiao, Eric Xing, Laurent El Ghaoui, and Michael Jordan. Theoretically principled trade-off between robustness and accuracy. In *International conference on machine learning*, pages 7472–7482. PMLR, 2019.
- [52] Qiyang Zhao and Lewis D Griffin. Suppressing the unusual: towards robust cnns using symmetric activation functions. *arXiv preprint arXiv:1603.05145*, 2016.

A Ablation Experiment

We conducted several experiments to evaluate the effectiveness of MeanSparse in various scenarios. In this section, we use APGD accuracy (accuracy after attacking the model with Auto-PGD using both Cross-entropy and Difference of Logits Ratio loss metrics) as the robustness metric [8]. During our simulations, we found APGD accuracy to be almost equal to AA accuracy, with the advantage that APGD can be measured faster.

A.1 Activation Function

MeanSparse is generally appended before the activations function. This questions the effectiveness of MeanSparse for different activation functions. In this experiment, we check the performance of MeanSparse when integrating the models with different activation functions. The specifications of this experiment are:

- Dataset: CIFAR-10 [21]
- Architecture: ResNet-18 [18]
- Optimizer: SGD (initial learning rate: 0.1, weight decay: 0.0005, momentum: 0.9)
- Number of Epochs: 200
- Batch Size: 256

- Learning rate scheduler: The initial learning rate of 0.1 is reduced by a factor of 10 at epoch 100 and 150.
- Best model selection: We evaluate the model at each epoch of training and select the one with the highest PGD adversarial accuracy on the test set.
- Adversarial training properties: 10 step PGD adversarial training [26] with respect to ℓ_∞ attacks with radius $8/255$ and step size of 0.0078.

The experiments were conducted using an NVIDIA A100 GPU. Training each ResNet-18 model required approximately 6 hours of computational time on a single A100 GPU. In addition, the evaluation of each trained model took around 20 minutes on the same GPU.

Table 2 demonstrates the Clean and APGD accuracy metrics for a base ResNet-18 model, denoted by *Base*, with different activation functions and the same model post-processed by the proposed pipeline to integrate MeanSparse. We use both non-parametric and parametric activation functions, such as PSSiLU [9]. In our experiment, the GELU activation function, proposed in [19] and generally used in attention-based architectures, results in the best APGD accuracy. When this model is integrated with MeanSparse, we observe a significant improvement in APGD accuracy (49.12% \rightarrow 50.37%) while the clean accuracy slightly decreases (84.59% \rightarrow 84.32%) for $\alpha = 0.2$. Additionally, if we can tolerate $\sim 1\%$ reduction in clean accuracy, we can increase APGD accuracy by more than 2%. The first important takeaway is the effectiveness of MeanSparse integration with different activations and the inability of the activation function to replicate the role of the MeanSparse technique. The second is that $\alpha = 0.2$ consistently leads to large improvements in APGD accuracy with a negligible reduction in clean accuracy for all activation functions. Even for the ReLU activation function, $\alpha = 0.2$ increases both Clean and APGD accuracies simultaneously. We will use the ResNet-18 model trained adversarially with GELU activation over the CIFAR-10 dataset for our future experiments.

Table 2: Clean and APGD accuracy of ResNet18 model with different activation functions over CIFAR-10 test set before (Base) and after integration with MeanSparse technique for different value of α

α	Activation											
	ReLU		ELU		GELU		SiLU		PSiLU		PSSiLU	
	Clean	APGD	Clean	APGD	Clean	APGD	Clean	APGD	Clean	APGD	Clean	APGD
Base	83.59	47.77	81.65	46.65	84.59	49.12	83.05	48.54	84.80	48.02	83.95	48.03
0.05	83.58	47.89	81.64	47.47	84.63	49.25	83.10	48.70	84.80	48.11	83.97	48.22
0.1	83.59	48.25	81.58	48.69	84.58	49.57	83.09	49.05	84.72	48.58	83.95	48.61
0.15	83.57	48.60	81.53	49.22	84.42	50.00	83.11	49.73	84.66	48.88	83.93	49.05
0.2	83.71	48.88	81.53	49.49	84.32	50.37	83.01	50.01	84.69	49.07	83.79	49.29
0.25	83.46	49.30	81.56	49.14	84.18	50.80	83.00	50.59	84.61	49.36	83.75	49.32
0.3	83.48	49.24	81.20	48.66	83.95	51.13	82.78	50.81	84.27	49.35	83.81	49.19
0.35	83.13	49.27	80.34	47.60	83.51	51.36	82.49	50.79	83.76	49.25	83.55	49.11
0.4	82.49	48.87	78.77	46.10	82.85	51.25	81.34	49.97	83.20	48.76	82.69	48.63

A.2 Threat Model

In this experiment, we focused on the effectiveness of MeanSparse against two well-studied threat models, ℓ_∞ and ℓ_2 . Until now, our focus was on the ℓ_∞ threat model, which generally results in lower robust accuracy [7]. On the other hand, ℓ_2 threat models can focus on a specific part of the image, and this localization of adversarial perturbation may challenge the effectiveness of the MeanSparse technique. In this experiment, we compare the robustness against both ℓ_∞ and ℓ_2 threat models. The model is ResNet18 with the GELU activation function as in our *Activation Function* experiment in 2. Table 3 illustrates the clean and APGD accuracy for ℓ_∞ and ℓ_2 threats. As the accuracy for the ℓ_∞ threat model increases with increasing α , the accuracy for ℓ_2 also increases, which depicts the effectiveness and generalization of MeanSparse across well-studied threat models. Additionally, the improvement compared to the base model at $\alpha = 0.2$ is larger for the ℓ_2 threat than for the ℓ_∞ threat.

Table 3: Clean and APGD accuracy of ResNet18 model with GELU activation function over CIFAR-10 test set before (Base) and after integration with MeanSparse technique for different value of α and different threat models from RobustBench [8]

α	Threat Model		
	Clean	$\ell_\infty, \epsilon = \frac{8}{255}$	$\ell_2, \epsilon = \frac{128}{255}$
		APGD	APGD
Base	84.59	49.12	59.98
0.05	84.63	49.25	60.23
0.10	84.58	49.57	60.53
0.15	84.42	50.00	60.87
0.20	84.32	50.37	61.36
0.25	84.18	50.80	61.60
0.30	83.95	51.13	61.73
0.35	83.51	51.36	61.74
0.40	82.85	51.25	61.74

A.3 Adversarial Training

MeanSparse is designed to integrate with models trained using adversarial training. In previous experiments, PGD [26] was used for adversarial training. In this section, we compare the PGD results with those of TRADES [51] for adversarial training. For TRADES adversarial training, we set $\beta = 0.6$. For the other properties of adversarial training, we adopt the parameters specified in Section 2. Table 4 compares the results for base adversarially trained models and models integrated with MeanSparse. For TRADES, MeanSparse can still improve the APGD accuracy while maintaining clean accuracy. This table demonstrates overlapping information gathered around the mean feature values for both PGD and TRADES as adversarial training methods. In both methods, the information around the feature mean with a value of $\alpha \simeq 0.2$ is almost uninformative for clean data but can be utilized by attackers. Thus, the performance of MeanSparse represents generalizability across both PGD and TRADES adversarial training methods.

Table 4: Clean and APGD accuracy of ResNet-18 model with GELU activation function over CIFAR-10 test set before (Base) and after integration with MeanSparse technique for different value of α and adversarial training based on PGD [26] and TRADES [51]

α	Adversarial training			
	PGD		TRADES	
	Clean	APGD	Clean	APGD
Base	84.59	49.12	83.01	47.03
0.05	84.63	49.25	83.04	47.16
0.10	84.58	49.57	83.09	47.61
0.15	84.42	50.00	83.11	48.08
0.20	84.32	50.37	83.08	48.64
0.25	84.18	50.80	83.02	48.92
0.30	83.95	51.13	82.92	49.34
0.35	83.51	51.36	82.62	49.24
0.40	82.85	51.25	82.20	48.76

A.4 Feature Centerization Type

The MeanSparse technique applies sparsification over mean-centered features across each channel in the input tensor to the activation function. In this section, we inspect the importance of the reference for feature centralization before sparsification in our proposed technique. For this purpose, we compare three cases where the reference for centering features is the channel mean (μ_{ch}), zero, and the mean over all features in all channels (μ). For a fair comparison across all cases, we select the sparsification threshold equal to $\alpha \times \sigma_{ch}$, where σ_{ch} emphasizes the channel-wise calculation standard deviation. Table 5 represents the result for different options of reference. When using zero as the reference for feature centralization, the improvement in APGD is higher than using the mean as the reference, but on the other hand, the utilization of the model also decreases. One challenging problem is the high rate of clean accuracy reduction when using zero as the reference, which may cause a huge reduction if not selected properly. When using the mean of all channels as the reference, the results in terms of both clean and APGD accuracy metrics underperform compared to the case where the channel mean is used as the reference. The main takeaway from the table is the importance of using channel-wise statistics to maintain utility while improving robustness.

Table 5: Clean and APGD accuracy of ResNet18 model with GELU activation function over CIFAR-10 test set before (Base) and after the application of MeanSparse technique for different references for feature centralization

α	Reference for Centralization					
	zero		μ		μ_{ch}	
	Clean	APGD	Clean	APGD	Clean	APGD
<i>Base</i>	84.59	49.12	84.59	49.12	84.59	49.12
0.05	84.58	49.32	84.58	49.22	84.63	49.25
0.1	84.50	49.63	84.52	49.45	84.58	49.57
0.15	84.30	50.26	84.36	49.79	84.42	50.00
0.2	84.06	50.98	84.13	50.23	84.32	50.37
0.25	83.55	51.58	83.83	50.73	84.18	50.80
0.3	82.81	52.08	83.27	50.87	83.95	51.13
0.35	81.68	51.95	82.52	50.61	83.51	51.36
0.4	79.84	51.72	81.09	49.93	82.85	51.25

A.5 Attack Power

In the previous experiments, the attack power was set to a fixed value of $8/255$ for ℓ_∞ attack threat which is generally the threshold of imperceptibility [8]. In this experiment, we explore the effectiveness of the MeanSparse technique for a wide range of attack powers. Table 6 represents the APGD accuracy for ϵ values starting from $1/255$ to $16/255$. For $\alpha = 0.2$, the accuracy is smaller than the base model ($\alpha = 0$) for $1/255$ and $2/255$ values of ϵ , which is generally due to the reduction of clean accuracy after applying MeanSparse (clean accuracy reduces to 84.32 from 84.59). For ϵ values larger than $2/255$, applying the MeanSparse technique persistently improves the APGD accuracy. The same trend is also observed for $\alpha = 0.35$ except for the fact that after $\epsilon = 4/255$, we have persistent improvements over the base model.

A.6 Applying to Specific Activation Functions

The MeanSparse technique is designed to sparsify mean-centered inputs to all activation functions in a model. In this experiment, we will focus on applying sparsification over a selected subset of activation functions. For this purpose, we index the activation functions in the ResNet18 model. This model has 8 residual blocks, each with 2 activation functions: one in the *Main Path* and one after the result of the main path is added to the residual connection, totaling 16 activation functions. Additionally, this architecture has one activation function before the residual block. So, in total, we have 17 indices. Index 0 is the initial activation function. The odd indices are related to the activation function in the main path, and the even indices correspond to activation functions after the addition of the residual

Table 6: APGD accuracy of ResNet18 model with GELU activation function over CIFAR-10 test set before (Base denoted by $\alpha = 0$ in the table) and after the application of MeanSparse technique for different attack power ϵ and two different α values (0.20 and 0.35). Clean accuracy is provided next to each α value.

ϵ	α		
	0 (84.59)	0.2 (84.32)	0.35 (83.51)
	APGD	APGD	APGD
1/255	81.10	80.97	79.60
2/255	77.72	77.60	76.47
3/255	73.37	73.54	72.64
4/255	68.88	69.08	68.80
5/255	64.31	64.70	64.48
6/255	58.95	59.92	60.15
7/255	54.11	55.15	55.71
8/255	49.12	50.37	51.36
9/255	42.77	44.41	45.72
10/255	37.48	39.17	40.77
11/255	32.62	34.20	36.04
12/255	28.12	29.77	31.50
13/255	23.77	25.44	27.18
14/255	19.42	20.76	22.77
15/255	15.51	17.01	19.09
16/255	11.97	13.41	15.44

connection to the main path output. We select two scenarios. In the first scenario, denoted by *Single Layer*, we present the results when MeanSparse is applied to only the corresponding row-indexed activation function, while *Cumulative* depicts the result when MeanSparse is applied to the activation functions with indices less than or equal to the index represented in each row.

One shared remark in both Single Activation and Cumulative cases is that the starting layers are more effective in improving robustness. We can attribute this to the abstraction level in different layers of the ResNet18 model. In the case of Single Activation, when we apply the MeanSparse technique to larger indices, we observe that not only does the robust accuracy decrease, but the clean accuracy increases. This indicates that for even better performance, we can use different α values for activation functions based on their depth level. Note that for the current version of the MeanSparse technique, we use a shared α for all activation functions.

Another aspect worth inspecting in this experiment is how the application of the MeanSparse technique to activation functions in the main path and after the addition of residual data to the main path result affects robustness in terms of APGD accuracy. So we consider two cases in Table 8. In the first case, MeanSparse is applied to all the activation functions in the main path of the ResNet block, denoted by *Main Path*. In the second case, MeanSparse is applied to all the activation functions after the addition of residual data to the output of the main path, denoted by *After Addition*. This table reveals an important result. While the application of MeanSparse to both types of activation functions contributes to the robustness of the model, the application of MeanSparse to the main flow of the model (*After Addition*) is more responsible for the improvements in the ranges where clean accuracy is almost unchanged ($\alpha \simeq 0.2$).

Table 7: Clean and APGD accuracy of ResNet18 model with GELU activation function over CIFAR-10 test set after the application of MeanSparse technique for *Single Activation* and *Cumulative* cases. Single Activation represents the results when MeanSparse is applied to only the index activation function, and Cumulative Activation represents the results when MeanSparse is applied to the index activation function and all previous activation functions (for the based model the Clean and APGD accuracy are 84.59% and 49.12%, respectively).

Index	Single Activation				Cumulative			
	Threshold		Threshold		Threshold		Threshold	
	0.2	0.35	0.2	0.35	0.2	0.35	0.2	0.35
	Clean	APGD	Clean	APGD	Clean	APGD	Clean	APGD
0	84.52	49.34	84.21	49.19	84.52	49.37	84.21	49.19
1	84.56	49.19	84.44	49.09	84.53	49.38	84.31	49.35
2	84.46	49.21	84.45	49.20	84.49	49.37	83.98	49.29
3	84.50	49.15	84.33	49.19	84.45	49.52	83.72	49.69
4	84.48	49.21	84.26	49.26	84.41	49.67	83.47	50.02
5	84.54	49.24	84.36	49.25	84.38	49.86	83.14	50.29
6	84.60	49.11	84.58	49.21	84.34	49.90	83.21	50.50
7	84.51	49.13	84.45	49.16	84.32	49.99	83.02	50.65
8	84.58	49.19	84.59	49.21	84.34	50.12	83.05	50.86
9	84.60	49.12	84.53	49.02	84.35	50.32	82.96	51.09
10	84.59	49.06	84.59	49.07	84.34	50.35	83.12	51.15
11	84.60	49.06	84.56	49.05	84.38	50.33	83.02	51.23
12	84.62	49.09	84.72	49.05	84.37	50.27	83.09	51.23
13	84.59	49.13	84.63	49.09	84.38	50.37	83.14	51.20
14	84.60	49.17	84.63	49.12	84.40	50.34	83.26	51.41
15	84.57	49.15	84.69	49.10	84.36	50.38	83.30	51.37
16	84.63	49.09	84.75	49.01	84.32	50.37	83.51	51.36

Table 8: Clean and APGD accuracy of ResNet18 model with GELU activation function over CIFAR-10 test set before (Base denoted by $\alpha = 0$ in the table) and after the application of MeanSparse technique for *Main Path* (application of MeanSparse to activation functions in the main path of residual block) and *After Addition* (application of MeanSparse to activation functions operating after addition of main path result and residual data) cases.

α	Layer type			
	Main Path		After Addition	
	Clean	APGD	Clean	APGD
Base	84.59	49.12	84.59	49.12
0.05	84.59	49.20	84.62	49.25
0.10	84.59	49.31	84.59	49.43
0.15	84.50	49.43	84.49	49.53
0.20	84.40	49.63	84.47	49.66
0.25	84.26	49.68	84.46	49.93
0.30	83.94	49.88	84.27	49.90
0.35	83.66	49.94	84.15	49.73
0.40	82.96	49.91	83.67	49.24